

## APPLICATION NOTE

### ICP - Mass Spectrometry

**Author:**

Chady Stephan

PerkinElmer, Inc.  
Shelton, CT

## Analysis of Iron Nanoparticles in Organic Solvents Used in the Semiconductor Industry Using Single Particle ICP-MS in Reaction Mode

### Introduction

Metallic contamination in semiconductor products adversely affects device performance. As line widths on chips decrease, the allowable levels of metal contamination also decrease. The most commonly occurring forms of metal contamination are either transition

metals or alkaline elements. Transition metals tend to diffuse through the semiconductor material and aggregate on the surface in various oxide forms. Among the transition metals, iron (Fe) is, by far, the most common contaminant.

Single particle ICP-MS (SP-ICP-MS) has proven to be a popular technique for the analysis of nanoparticles due to its ability to detect, count, and size individual particles at very low particle concentrations down to limits between 100 and 1000 particles/mL, depending on the introduction system being used. Along with the particulate information, SP-ICP-MS will provide the user with the dissolved concentration without prior separation<sup>1</sup>. Many available publications have demonstrated the ability of SP-ICP-MS to measure and characterize nanoparticles in a wide variety of matrices<sup>2-5</sup>, including chemical mechanical planarization slurries<sup>6</sup>.

Iron ( $^{56}\text{Fe}^+$ ) is known to exhibit plasma-based interferences, more specifically  $^{40}\text{Ar}^{16}\text{O}^+$ . Dynamic Reaction Cell™ (DRC) technology, along with the use of ammonia as a reactive gas, is the most efficient way to remove the  $\text{ArO}^+$  interference on the most abundant isotope of Fe ( $^{56}\text{Fe}^+$ ), which is required to achieve the lowest Fe-nanoparticle size detection limits<sup>7</sup>.

This work will demonstrate the ability to measure and characterize Fe nanoparticles and iron oxides in semiconductor solvents using SP-ICP-MS in Reaction mode.

## Experimental

### Reagents and Sample Preparation

Iron oxide ( $\text{Fe}_2\text{O}_3$ ) – PVP capped nanoparticles of  $20 \text{ nm} \pm 5 \text{ nm}$  were purchased from nanoComposix™ (San Diego, California, USA) and used as a quality control (QC) sample. Transport efficiency was determined using 60 nm gold (Au) nanoparticles prepared in each analyzed solvent at a concentration of 50,000 particles/mL (Note: transport efficiency is independent of particle size). Dissolved Fe standards (100, 200, and 300 ppt) were prepared in 1% nitric acid and a certain % of isopropyl alcohol (IPA). Nitric acid was necessary to keep iron from precipitating, while IPA was added to compensate for the difference in both the ionization potential and transport efficiency between the aqueous standards and the solvents (i.e. samples) being analyzed. The level of added IPA was assessed based on the sample matrices being analyzed. All nanoparticle solutions were sonicated for 10 minutes prior to analysis.

Samples included tetramethylammonium hydroxide (TMAH) and mixture of 90% cyclohexane / 10% propylene glycol monomethyl ether (PGME).

### Instrumental Conditions

All analyses were performed on a PerkinElmer NexION® 350S ICP-MS using the Syngistix™ Nano Application Software Module (Version 1.1). Instrumental conditions are shown in Table 1. The sample introduction conditions varied slightly depending on which solvent was analyzed, with oxygen added after the spray chamber to prevent carbon deposition on the cones. All other components and parameters remained constant.

Table 1. NexION 350S ICP-MS Instrumental Parameters.

Parameter	Value
Nebulizer	PFA, self-aspirating
Sample Uptake Rate	0.112 mL/min (TMAH) 0.515 mL/min (cyclohexane, PGME)
Spray Chamber	PC3
Spray Chamber Temperature	+2 °C
Oxygen Flow	0.05 L/min
Injector	0.85 mm ID, quartz
RF Power	1600W
Analyte	Fe at m/z 56
Reaction Gas	$\text{NH}_3$
RPq	0.65 (TMAH, cyclohexane, PGME)
Dwell Time	50 $\mu\text{s}$
Analysis Time	60 s

## Results and Discussion

Before organic solvents were analyzed, the performance of the instrument for Fe nanoparticles in aqueous solutions was evaluated. Since the interference on  $^{56}\text{Fe}^+$  ( $\text{ArO}^+$ ) is present whether aqueous or organic solvents are analyzed, the optimum  $\text{NH}_3$  flow was established by running 20 nm  $\text{Fe}_2\text{O}_3$  nanoparticles at various  $\text{NH}_3$  flows. The resulting mean intensity counts from the nanoparticles and the dissolved intensity counts were recorded, and the signal-to-background (S/B) ratios calculated. Figure 1 shows a plot of the ammonia optimization, indicating an optimal ammonia flow of 0.5-0.6 mL/min ( $\text{S/B} = 260$ ), demonstrating the effectiveness of ammonia in removing the  $\text{ArO}^+$  interference while retaining  $\text{Fe}^+$  sensitivity. All analyses were done with an  $\text{NH}_3$  flow of 0.55 mL/min.

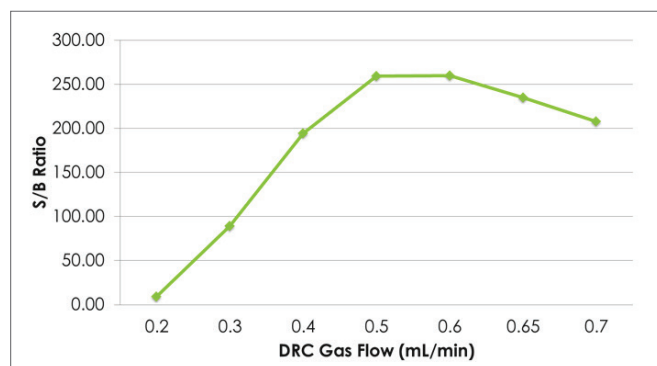


Figure 1. Ammonia flow optimization for 30 nm  $\text{Fe}_2\text{O}_3$  nanoparticles in water.

With the optimum ammonia flow established, the feasibility of analyzing Fe nanoparticles was determined by analyzing 20 nm  $\text{Fe}_2\text{O}_3$  nanoparticles in water. Figure 2 shows the particle size distributions at a concentration of 50,000 particles/mL. As shown in Table 2, the average measured sizes (20 nm) agree with the certificate values ( $20 \pm 5 \text{ nm}$ ), validating that Fe-containing nanoparticles can be accurately measured using SP-ICP-MS in Reaction mode using ammonia as a reactive gas. In addition, the precision of the measurements is less than 3%.

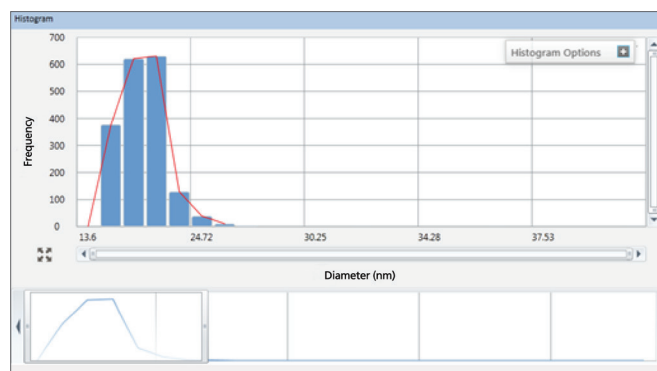


Figure 2. Size distribution of 20 nm  $\text{Fe}_2\text{O}_3$  prepared in 1% IPA.

Table 2. Accuracy and Precision of 20 nm Fe<sub>2</sub>O<sub>3</sub> Nanoparticle Analysis at m/z 56.

Replicate	Most Frequent Size (nm)	Mean Size (nm)	Particle Conc. (part/mL)
20 nm Fe <sub>2</sub> O <sub>3</sub> - 1	19.6	20.2	50801
20 nm Fe <sub>2</sub> O <sub>3</sub> - 2	20.6	20.3	51075
20 nm Fe <sub>2</sub> O <sub>3</sub> - 3	19.6	20.1	50862
20 nm Fe <sub>2</sub> O <sub>3</sub> - 4	20.1	20.7	50926
<i>Average</i>	<i>20.0</i>	<i>20.3</i>	<i>50916</i>
<i>Std. Dev.</i>	<i>0.47</i>	<i>0.28</i>	<i>117</i>
<i>RSD</i>	<i>2.35%</i>	<i>1.36%</i>	<i>0.23%</i>

To determine size detection limits for Fe nanoparticles, deionized water blanks were analyzed which did not contain any Fe nanoparticles. The resulting background noise corresponds to 13 nm particles. Table 3 shows the detection limits from three analyses, along with the counts of dissolved Fe determined in the same analysis. The low intensity for dissolved iron demonstrates that ArO<sup>+</sup> is eliminated in Reaction mode and that there is very little Fe contamination in the sample. The reproducibility of the results indicates that these are real detection limits and not the result of random signals.

Table 3. Size Detection Limits for Iron Nanoparticles in Water.

Replicate	Most Frequent Size (nm)	Mean Size (nm)	Dissolved Intensity (counts)
1	13.7	13.7	0.14
2	13.0	13.4	0.14
3	12.9	12.9	0.14
<i>Average</i>	<i>13.2</i>	<i>13.3</i>	<i>0.14</i>
<i>Std. Dev.</i>	<i>0.44</i>	<i>0.40</i>	<i>&lt; 0.01</i>
<i>RSD</i>	<i>3.30%</i>	<i>3.03%</i>	<i>&lt; 0.01</i>

With feasibility established, the methodology was applied to the solvents for Fe-containing nanoparticles. To determine the background, a mixture of deionized water and 10% PGME was analyzed. The resulting real-time scan appears in Figure 3, which shows no Fe-containing nanoparticles being detected.

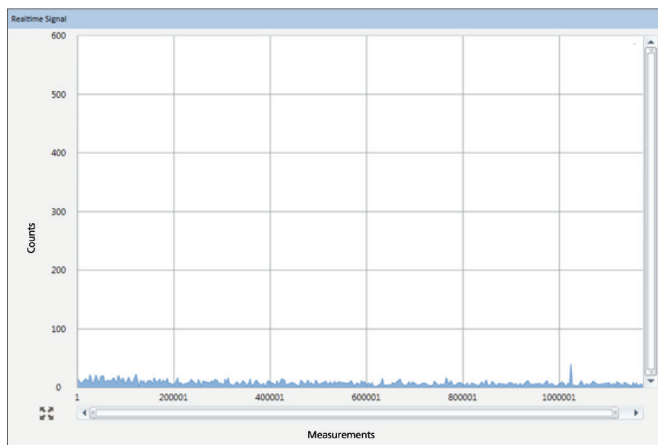


Figure 3. Real-time display from the analysis of 20% PGME in deionized water showing that no Fe-containing nanoparticles are detected.

The cyclohexane (90% cyclohexane + 10% PGME) mixture was then analyzed, and the real-time display showed numerous Fe-containing nanoparticles, as seen as spikes in Figure 4. These nanoparticles must originate from the cyclohexane as the 10% mixture of PGME did not show any nanoparticles (Figure 3). This result proves that Fe-containing nanoparticles can be detected in organic solvents.

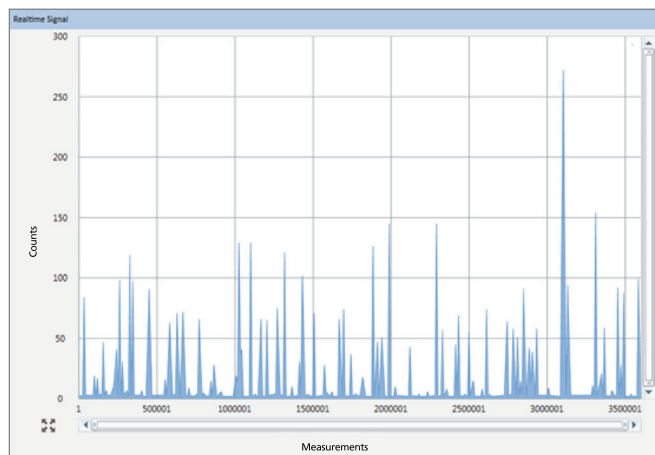


Figure 4. Real-time display from the analysis of 90% cyclohexane + 10% PGME showing Fe-containing nanoparticles.

The corresponding particle size and concentration results from three analyses of the sample appear in Table 4 and demonstrate the consistency of the methodology, both for the measured size and particle concentration, even at very low particle concentrations.

Table 4. Fe Particle Size and Concentration from the Analysis of 90% Cyclohexane and 10% PGME.

Sample	Most Frequent Size (nm)	Mean Size (nm)	Particle Concentration (particles/mL)
1	59.0	92.8	2971
2	60.7	89.8	2929
3	63.0	89.7	2935
<i>Average</i>	<i>60.9</i>	<i>90.8</i>	<i>2945</i>
<i>Std. Dev.</i>	<i>2.01</i>	<i>1.76</i>	<i>22.7</i>
<i>RSD</i>	<i>3.30%</i>	<i>1.94</i>	<i>0.77</i>

The calculated particle size depends on both the density of the particles and the particle composition (mass fraction of iron). Table 5 shows the same results as in Table 4, but under two different assumptions: that the particles are pure Fe and that they are stainless steel particles. As the data shows, the sizes vary slightly.

Table 5. Fe Nanoparticle Size in 90% Cyclohexane/10% PGME under Two Different Assumptions.

Composition	Sample	Most Frequent Size (nm)	Mean Size (nm)
<i>Metallic Fe</i> Density = 7.87 g/cm <sup>3</sup> Fe Mass Fraction: 100%	1	59.0	92.8
	2	60.7	89.8
	3	63.0	89.7
<i>Stainless Steel</i> Density = 7.70 g/cm <sup>3</sup> Fe Mass Fraction: 70%	1	67.0	105
	2	68.8	102
	3	71.5	94.9

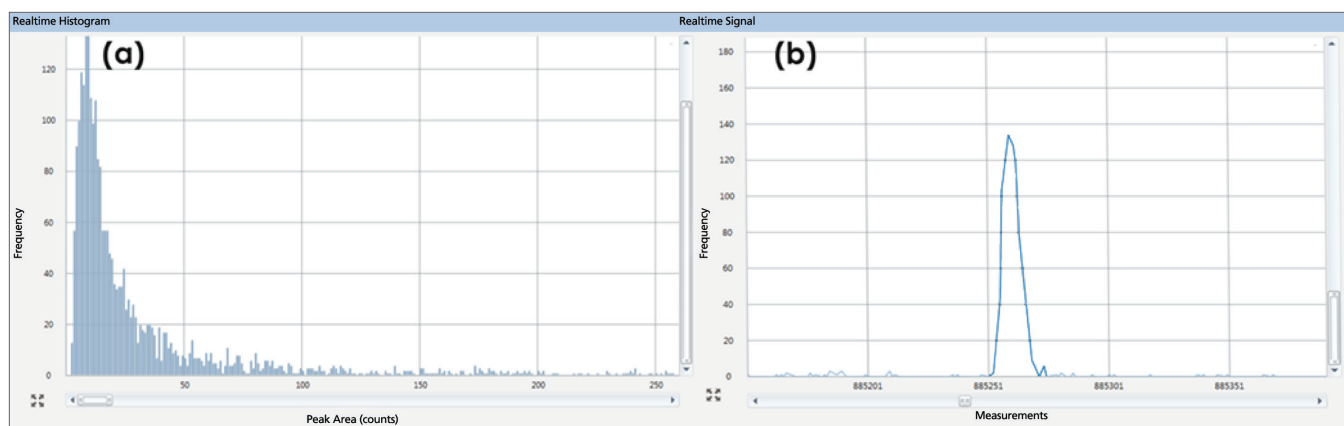


Figure 5. Fe-containing nanoparticle in TMAH. (a) Particle size distribution. (b) Real-time signal from a single Fe-containing nanoparticle.

Next, TMAH diluted ten times with deionized water was analyzed, with the results appearing in Figure 5 and Table 6. Figure 5a shows the particle size distribution on the left, while the signal from a single Fe nanoparticle appears in Figure 5b. (The x-axis in Figure 5b is zoomed significantly to show the single peak.) As with the cyclohexane, the results are consistent over three replicate analyses, both for particle size and concentration. Table 6 shows the results from three analyses of the sample, which again demonstrate the consistency of the methodology, both for particle size and concentration.

To determine if these nanoparticles originate from stainless steel, the sample was run again, this time monitoring chromium (Cr). As the real-time trace in Figure 6 shows, no particles are present, which means that these Fe-containing nanoparticles are not stainless steel. Based on TMAH chemistry, it is suspected that these are  $\text{Fe}(\text{OH})_2$  particles.

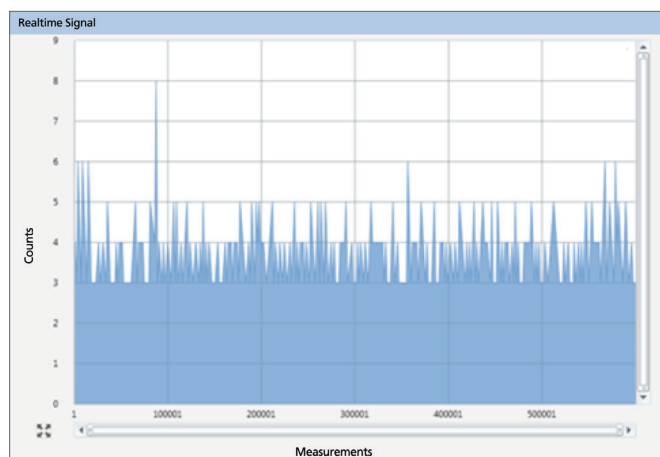


Figure 6. Real-time signal for Cr-containing nanoparticles in TMAH. Since no Cr-containing particles are detected, the Fe-containing particles detected in Figure 5 cannot be from stainless steel.

Assuming that  $\text{Fe}(\text{OH})_2$  particles are present in the TMAH, the total iron concentration being measured can be calculated based on the density of  $\text{Fe}(\text{OH})_2$ , ( $3.4 \text{ g/cm}^3$ ), the Fe mass fraction (70%), the particle size, and particle concentration. Table 7 displays the data for three replicate analyses of the TMAH, which shows that the total concentration of iron (converted from the particle concentration and assuming particles are clusters of  $\text{Fe}(\text{OH})_2$ ) is being detected with great precision.

Table 7 displays the data for three replicate analyses of the TMAH and shows the total concentration of iron detected after conversion from the particle concentration and assuming particles are clusters of  $\text{Fe}(\text{OH})_2$ .

Table 6. Fe Nanoparticle Size and Concentrations in TMAH.

Sample	Most Frequent Size (nm)	Particle Conc. (particles/mL)	Dissolved Intensity (counts)
1	27.6	43809	0.11
2	26.6	43253	0.08
3	26.9	42617	0.08
Average	27.0	43226	0.09
Std. Dev.	0.513	596	0.02
RSD	1.90%	1.38%	19.2%

Table 7. Mass Conversion of Fe from  $\text{Fe}(\text{OH})_2$  to total Fe.

Sample	Mean Size (nm)	Particle Conc. (part/mL)	Mass of individual $\text{Fe}(\text{OH})_2$ particle (g)	Fe Concentration (ppt)
1	41.6	43809	$1.28\text{E-}16$	3.92
2	41.0	43253	$1.23\text{E-}16$	3.71
3	40.0	42617	$1.14\text{E-}16$	3.40
Average	40.9	43226	0.00	3.68
Std. Dev.	0.80	596	$7.09\text{E-}18$	0.262
RSD	1.98%	1.38%	5.83%	7.11%

## Conclusion

This work has demonstrated the ability of SP-ICP-MS in Reaction mode to detect Fe-containing nanoparticles in organic solvents. By using ammonia in Reaction mode on the NexION 350, the  $\text{ArO}^+$  interference on the main isotope of Fe ( $m/z$  56) is completely eliminated, allowing the size and concentration of Fe-containing nanoparticles to be accurately determined. Reaction mode was used instead of Collision mode since the latter cannot eliminate the  $\text{ArO}^+$  interference without causing a significant sensitivity loss for iron, which would prevent the Fe-containing nanoparticles from being seen. In Reaction mode, Fe nanoparticle detection limits of 13 nm were established, and particles were accurately counted and sized at concentrations as low as 3000 particles/mL in organic solvents. Future work will focus on other nanoparticles which will benefit from Reaction mode.

## Consumables Used

Component	Part Number
60 nm Spherical Au Nanoparticles	N8142303 (25 mL)
PerkinElmer Pure-Grade Standard, 1000 ppm	N9303771 (125 mL) N9300126 (500 mL)
Sample Tubes	B0193233 (15 mL) B0193234 (50 mL)

## References

1. Stephan, C., Neubauer, K. "Single Particle Inductively Coupled Plasma Mass Spectrometry: Understanding How and Why", PerkinElmer white paper, 2014.
2. Hadioui, M., Wilkinson, K., Stephan, C. "Assessing the Fate of Silver Nanoparticles in Surface Water using Single Particle ICP-MS", PerkinElmer application note, 2014.
3. Donovan, A.R., Shi, H., Adams, C., Stephan, C. "Rapid Analysis of Silver, Gold, and Titanium Dioxide Nanoparticles in Drinking Water by Single Particle ICP-MS", PerkinElmer application note, 2015.
4. Neubauer, K., Stephan, C., Kobayashi, K. "Analysis of  $\text{SiO}_2$  Nanoparticles in Standard Mode with Single Particle ICP-MS", PerkinElmer application note, 2015.
5. Gray, E., Higgins, C.P., Ranville, J.F. "Analysis of Nanoparticles in Biological Tissues using SP-ICP-MS", PerkinElmer application note, 2014.
6. Davidowski, L., Stephan, C. "The Characterization of Nanoparticle Element Oxide Slurries Used in Chemical-Mechanical Planarization by Single Particle ICP-MS", PerkinElmer application note, 2014.
7. Ong, K. "Determination of Impurities in Organic Solvents used in the Semiconductor Industry with the NexION 300/350S ICP-MS", PerkinElmer application note, 2012-2014.